THE JOURNAL OF BIOLOGICAL CHEMISTRY VOL. 285, NO. 52, pp. 40706–40713, December 24, 2010

Molecular Association of the *Arabidopsis* ETR1 Ethylene Receptor and a Regulator of Ethylene Signaling, RTE1*[S]

Received for publication, May 19, 2010, and in revised form, October 11, 2010 Published, JBC Papers in Press, October 15, 2010, DOI 10.1074/jbc.M110.146605

Chun-Hai Dong[‡], Mihue Jang[§], Benjamin Scharein[¶], Anuschka Malach[¶], Maximo Rivarola[‡], Jeff Liesch[‡], Georg Groth[¶], Inhwan Hwang[§], and Caren Chang[‡1]

From the [‡]Department of Cell Biology and Molecular Genetics, University of Maryland, College Park, Maryland 20742, the [§]Division of Integrative Biosciences and Biotechnology and Division of Molecular and Life Sciences, Pohang University of Science and Technology, Pohang, 790-784 Korea, and the [¶]Department of Plant Biochemistry, Heinrich-Heine Universität, 40225 Düsseldorf, Germany

The plant hormone ethylene plays important roles in growth and development. Ethylene is perceived by a family of membrane-bound receptors that actively repress ethylene responses. When the receptors bind ethylene, their signaling is shut off, activating responses. *REVERSION-TO-ETHYLENE SENSITIVITY* (*RTE1*) encodes a novel membrane protein conserved in plants and metazoans. Genetic analyses in *Arabidopsis thaliana* suggest that RTE1 promotes the signaling state of the ethylene receptor ETR1 through the ETR1 N-terminal domain. RTE1 and ETR1 have been shown to co-localize to the endoplasmic reticulum (ER) and Golgi apparatus in *Arabidopsis*. Here, we demonstrate a physical association of RTE1 and ETR1 using *in vivo* and *in vitro* methods. Interaction of RTE1 and ETR1 was revealed *in vivo* by bimolecular fluorescence complementation (BiFC) in a tobacco cell transient assay and in stably transformed *Arabidopsis*. The association was also observed using a truncated version of ETR1 comprising the N terminus (amino acids 1–349). Interaction of RTE1 and ETR1 was confirmed by co-immunoprecipitation from *Arabidopsis*. The interaction occurs with high affinity (K_d, 117 nM) based on tryptophan fluorescence spectroscopy using purified recombinant RTE1 and a tryptophan-less version of purified recombinant ETR1. An amino acid substitution (C161Y) in RTE1 that is known to confer an *ETR1* loss-of-function phenotype correspondingly gives a nearly 12-fold increase in the dissociation constant (K_d, 1.38 μM). These findings indicate that a high affinity association of RTE1 and ETR1 is important in the regulation of ETR1.

The gaseous plant hormone ethylene is important in regulating many aspects of growth and development, including fruit ripening, senescence, abscission, and stress responses (1). There are a number of known components in ethylene signaling that form a pathway starting with the perception of ethylene and leading to gene expression changes (2, 3). *Arabidopsis thaliana* has five homologous ethylene receptors with sequence similarity to histidine protein kinase receptors (4–7). The receptors appear to be largely redundant in ethylene signaling, although the ETR1 ethylene receptor has a more predominant role (8–10). The N terminus of the ethylene receptors comprises an ethylene-binding domain (11–13) consisting of three membrane-spanning domains localized at the endoplasmic reticulum (ER) (14–16) and the Golgi apparatus (16). The cytosolic portion of the receptors exhibits histidine and/or serine/threonine protein kinase activity *in vitro* (17, 18) and control of autokinase activity by ethylene was demonstrated by *in vitro* phosphorylation studies using purified full-length ETR1 (19). However, the molecular mechanism of ethylene receptor signaling is still unknown, particularly as protein kinase activity appears to be largely dispensable for ethylene receptor signaling (8, 9).

The ethylene receptors are negative regulators of ethylene response, repressing responses in the absence of ethylene (10, 20) with the N-terminal domain controlling the signaling state of the receptor (21). When ethylene is bound, a conformational change presumably occurs within the receptor to turn off its signaling. Dominant gain-of-function mutations in any of the receptor genes encode amino acid substitutions in the N-terminal domain that cause the receptor to signal constitutively, resulting in dominant ethylene insensitivity (21).

The ethylene receptors are disulfide-linked homodimers (12, 22, 23) and form higher order multimeric complexes through non-covalent interactions (15, 23, 24). The five *Arabidopsis* ethylene receptors can form both homomeric and heteromeric complexes (23), and protein-protein interactions have been detected for all possible receptor combinations (15, 24). It is thought that higher order clustering allows for conformational changes within one receptor to be propagated to other receptors in the cluster, providing a mechanism for signal amplification.

The *Arabidopsis REVERSION-TO-ETHYLENE SENSITIVITY* 1 (*RTE1*)[2] gene is a positive regulator of *ETR1* that was

* This work was supported, in whole or in part, by Grant 1R01GM071855 from the National Institutes of Health (to C. C.), a grant from the World Class University project of the Ministry of Education, Science and Technology, Korea (to I. H.), and a grant of the Deutsche Forschungsgemeinschaft (to G. G.) within the SFB 590 "Inhärente und adaptive Differenzierungsprozesse" at the Heinrich-Heine-Universität Düsseldorf.

[S] The on-line version of this article (available at http://www.jbc.org) contains supplemental Table S1 and Figs. S1–S3.

[1] Supported in part by the University of Maryland Agricultural Experiment Station. To whom correspondence should be addressed: Dept. of Cell Biology and Molecular Genetics, Bioscience Research Bldg., University of Maryland, College Park, MD 20742-5815. Fax: 301-314-1248; E-mail: carenc@umd.edu.

[2] The abbreviations used are: RTE, *REVERSION-TO-ETHYLENE SENSITIVITY*; BiFC, bimolecular fluorescence complementation; CaMV, Cauliflower Mosaic Virus; LB, Luria-Bertani; MS, Murashige & Skoog salt formula; YFP, yellow fluorescent protein.

identified in a genetic screen for suppressors of the dominant *etr1-2* receptor mutant (25). *rte1* loss-of-function mutants display ethylene hypersensitivity similar to *etr1* loss of function mutants. Interestingly, some dominant *etr1* alleles, such as *etr1-2*, are highly dependent on *RTE1* to confer ethylene insensitivity, while other dominant *etr1* alleles, such as *etr1-1*, are largely or entirely *RTE1* independent (26). All of these dominant alleles encode amino acid substitutions within the ETR1 N-terminal domain, leading to speculation that the basis for *RTE1* dependence/independence may be related to the specific conformation of the ETR1 N terminus. Unexpectedly, RTE1 is highly specific for ETR1 and has no apparent role in the signaling of the four other *Arabidopsis* ethylene receptors (25, 27, 28).

RTE1 encodes a novel protein carrying two to four predicted transmembrane domains (25). RTE1 is highly conserved in plants and metazoans. Homologs all carry a domain of unknown function called DUF778, which is also found in some protists and fungi. The only functional insight into this protein family comes from ethylene signaling in plants, and the only known target of RTE1 action is the ETR1 ethylene receptor. The *Arabidopsis* genome carries a second copy of *RTE1*, called *RTE1-HOMOLOG* (*RTH*), but *RTH* does not appear to play the same role as *RTE1* in ethylene signaling.[3] Overexpression of a tomato *RTE1* homolog, *GREEN-RIPE*, confers inhibition of tomato fruit ripening along with other ethylene-insensitive phenotypes (29). Likewise, *RTE1* overexpression in *Arabidopsis* confers ethylene insensitivity (25, 28). This insensitivity is partially blocked by an *etr1*-null mutation, but is restored by expression of the ETR1 N terminus (residues 1–349), indicating that the ETR1 N terminus (residues 1–349) is the downstream target of RTE1 action (28).

RTE1 is found in the microsomal fraction[3] and co-localizes with ETR1 at the ER and Golgi apparatus (16). This report demonstrates a physical interaction of the RTE1 protein with the ETR1 receptor both *in vivo* and *in vitro*, examining the specificity of the interaction and the effects of *rte1* and *etr1* mutations. This work advances our understanding of RTE1 function and indicates that a physical association of RTE1 and the ETR1 receptor may be important for the regulation of ETR1 in ethylene signaling.

EXPERIMENTAL PROCEDURES

Plant Growth and Plant Transformation—Wild-type *Arabidopsis thaliana* (ecotype Columbia (Col-0)) and *Nicotiana benthamiana* were grown in soil under 16-h light/8-h dark in a controlled environment chamber at 20 °C under white fluorescent light. For protein extraction, seedlings were germinated on 1× MS plates for 3 days in the dark at 20 °C.

Stably transformed *Arabidopsis* plants were generated by the floral dip infiltration method mediated by *Agrobacterium tumefaciens* strain *GV3101* (30). To select for transformants, seedlings were either grown on 1× MS plates containing hygromycin 25 mg/liter or grown in soil and sprayed with Basta (0.033% Liberty Herbicide, Bayer Cropscience).

Agroinfiltration of tobacco leaves was carried out as previously described (31). *A. tumefaciens* strain C58C1 (pCH32) was grown in LB-broth supplemented with 5 mg/liter tetracycline and 100 mg/liter rifampicin. To enhance transgene expression, we co-infiltrated with *Agrobacterium* carrying the p19 suppressor of gene silencing (31) grown in LB-broth supplemented with 50 mg/liter kanamycin. For infiltration, 50-ml cultures of *Agrobacterium* in LB-broth supplemented with 10 mM MES and 20 mM acetosyringone were precipitated, washed, and resuspended in a solution containing 10 mM MgCl, 10 mM MES and 100 mM acetosyringone. Tobacco leaves from 3-week-old plants were used for infiltration. Ten plants (two leaves per plant) were infiltrated per experiment.

Plasmid Construction for Bimolecular Fluorescence Complementation (BiFC) and Co-immunoprecipitation (co-IP)—See supplemental Table S1 for a list of all primers that were used to construct and/or mutagenize the DNA clones described below. To construct the binary vector expressing the cYFP-RTE1 fusion, we first used PCR to simultaneously amplify and fuse the full-length *RTE1* coding sequence downstream of the *cYFP* sequence, which encodes the C-terminal portion of YFP (amino acids 156–239), using an *RTE1* cDNA clone and the *pSPYCE-35S/pUC-SPYCE* vector (Walter *et al.*, Ref. 33) as respective templates. The *cYFP-RTE1* gene fusion fragment was cloned into the Gateway entry vector *pDONR221* using the Gateway recombination system (Invitrogen). The *cYFP-RTE1* gene fusion in *pDONR221* was verified by DNA sequencing and then transferred into the Gateway binary vector *pH2GW7* (32), which contains the *CaMV 35S* promoter, to produce *pH2GW7-cYFP-RTE1.* For the *rte1-1* mutant version encoding the C161Y substitution, the corresponding G-to-A mutation was introduced into the above *pH2GW7-cYFP-RTE1* construct by site-directed *in vitro* mutagenesis using the QuikChange kit (Stratagene) to produce *pH2GW7-cYFP-rte1-1.* For RTH, the binary vector expressing the cYFP-RTH fusion was constructed in the same way as cYFP-RTE1, using the *RTH* coding sequence in place of *RTE1*.

To generate the constructs encoding the ETR1-nYFP and ETR1(1–349)-nYFP fusions, the coding sequences for full-length *ETR1* and truncated *ETR1* (encoding amino acids 1–349) were each PCR-amplified from an existing ETR1 cDNA template (16), cloned into *pDONR221*, verified by DNA sequencing, and then transferred into the binary vector *pSPYNE-35S-GW* (33) using the Gateway system. The *etr1-1* and *etr1-2* full-length coding sequences were cloned into *pSPYNE-35S-GW* by the same strategy from existing cDNA clone templates.[4] Gene fusions of *ECA1-nYFP* and *ERS1-nYFP* in *pSPYNE-35S-GW* were cloned in the same way as *ETR1-nYFP*, using *ERS1* and *ECA1* coding sequences, respectively, in place of *ETR1*.

To create the construct encoding nYFP-ETR1, we first cloned the *ETR1* coding sequence into *pSPYNE-35S/pUC-SPYNE* (33) using restriction enzymes *Asc*I and ClaI. Since *pSPYNE-35S/pUC-SPYNE* carries nYFP downstream of the

[3] C. Chang, unpublished data.

[4] M. Rivarola and C. Chang, unpublished data.

cloning site, and we wanted an N-terminal fusion, we removed the C-terminal nYFP from the resulting construct using restriction enzymes XmaI and SstI. Next we PCR-amplified nYFP using *pSPYNE-35S/pUC-SPYNE* as a template and then cloned the amplified nYFP fragment using XbaI and *Asc*I at the N terminus of ETR1 within the altered *pSPYNE-35S/pUC-SPYNE* construct. The fusion was confirmed by DNA sequencing. The *nYFP-ETR1* gene fusion was then PCR-amplified and cloned into *pDONR221* and subsequently transferred into *pH2GW7* using the Gateway system.

To generate the construct encoding HA-RTE1 for co-IP, the full-length *RTE1* coding sequence was first cloned into *pDONR221*, verified by DNA sequencing, and then cloned between the *CaMV 35S* promoter and hemagglutinin epitope (HA) tag in the binary vector *pEarleyGate201* (34) using the Gateway system.

Fluorescence Microscopy—Imaging of YFP fluorescence in tobacco leaf or *Arabidopsis* seedlings was conducted under a laser scanning confocal microscope (Zeiss LSM510). The excitation wavelength used for YFP was 488 nm, and the emission filter wavelength was 520–550 nm. For visualization, tobacco leaf pieces or cotyledons and root fragments of *Arabidopsis* seedlings were directly mounted on glass slides in a drop of water. For each experiment, at least ten different samples were examined under the laser scanning microscope. Experiments were repeated three times.

Co-immunoprecipitation (co-IP)—To check the expression levels of the two constructs used for co-IP, we isolated the membrane fraction of *Arabidopsis* and carried out SDS-PAGE and Western blotting as previously described (16). For co-IP, 3-day-old dark-grown seedlings were homogenized in extraction buffer (250 mM sucrose, 25 mM Hepes-KOH, pH 7.5, 10 mM $MgCl_2$, 1 mM DTT, 1% Triton X-100) with protease inhibitors. The homogenate was sonicated (20 times) at 6 watts using a Model 100 Sonic Dismembrator (Fisher Scientific) and incubated at 4 °C for 3 h. The homogenate was then centrifuged at 2451 g for 10 min to remove debris. The protein extract was incubated with anti-HA monoclonal antibody (Roche Applied Science) in 2× IP buffer (25 mM HEPES-KOH, pH 7.5, 100 mMNaCl, 0.5 mM EDTA, 3 mM $MgCl_2$) at 4 °C for 4 h followed by additional incubation at 4 °C for 6 h with protein A-Sepharose beads. The beads were washed three times in IP buffer with 1% Triton X-100. Protein was eluted from the beads and separated by 10% SDS-PAGE followed by immunoblotting using anti-c-Myc (A-14) polyclonal (Santa Cruz Biotechnology or Roche Applied Science), anti-HA monoclonal, anti-SYP21 or anti-SYP61 antibodies (35, 36). To demonstrate that the extract used for co-IP was free of non-solubilized microsome vesicles (*i.e.* contained fully solubilized protein), similarly prepared extracts were subjected to ultracentrifugation, and then the pellet and soluble fractions were analyzed by immunoblotting (supplemental data Fig. S1).

Cloning, Expression, and Purification of Arabidopsis ETR1, RTE1, and RTE1-1 in E. coli—For ETR1, we used the existing clone pET16b-ETR1, which encodes a tryptophan-less ETR1 (with phenylalanine or leucine substituting for the endogenous tryptophan residues at positions 11, 53, 74, 182, 265, 288, and 563) (37, 38). The tryptophan-less ETR1 was expressed in *Escherichia coli* and purified as previously described (37, 38). To clone the full-length *RTE1* coding sequence into expression vector pET15b (Novagen), PCR was used to amplify the *RTE1* coding sequence with flanking NdeI and BamHI restriction sites using pDONR221-RTE1 as the template. The amplified fragment was then cloned into the pET15bvector at the NdeI and BamHI cloning sites and verified by sequencing. The RTE1-1 mutant version was created by *in vitro* site-directed mutagenesis of the wild-type *RTE1* template in pET15b. Using PCR, a fragment was amplified using an *rte1-1* mutagenesis primer as the forward primer together with a reverse primer that anneals to the vector. The PCR product itself was then used as a reverse primer with a forward primer using pET15b-RTE1 as template. The final product was cleaved with NdeI and BamHI and ligated into the pET15b vector digested with NdeI and BamHI. The clones were verified by nucleotide sequencing. The primer sequences used for cloning and mutagenesis are shown in supplemental Table S1. The resulting plasmids pET15b-RTE1 and pET15b-RTE1-1 each containing an N-terminal hexahistidine tag were transformed into *E. coli* strain BL21 Gold (DE3). Cultures were grown at 30 °C and expression of RTE1 or RTE1-1 was induced by the addition of 0.3 mM IPTG (isopropyl β-D-thiogalactoside) at an optical density of 0.7. Cells were harvested 4 h after induction by centrifugation and stored at −70 °C. The cell pellet was resuspended in 30 mM Tris-sulfate, pH 7.5, 200 mM NaCl, 0.002% (w/v) PMSF (phenylmethylsulfonyl fluoride) and passed through a French pressure cell at 12.000 psi. After centrifugation at 100,000 × *g* for 60 min the pellet was resuspended in the same buffer. RTE1 (or RTE1-1) was solubilized at room temperature by the addition of 1% (w/v) FOS-CHOLINE®-15(Anatrace). Unsolubilized material was removed by centrifugation at 100,000 × *g*. The supernatant was applied to a Ni-IDA (nickel-iminodiacetic acid) affinity column (0.5 cm diameter × 7 cm length) previously equilibrated with 30 mM Tris-Sulfate, pH 7.5, 200 mM NaCl, 0.002% (w/v) PMSF, and 0.05% (w/v) FOS-CHOLINE®-15. The column was washed with 30 bed volumes of the same buffer containing increasing concentrations of imidazole (25–100 mM) to remove contaminating proteins. Bound RTE1 or (RTE1-1) was eluted with 10 column volumes of the same buffer containing 250 mM imidazole. The imidizole concentration of the purified RTE1 (or RTE1-1) was decreased to 25 mM by adding 30 mM Tris-sulfate, pH 7.5, 200 mM NaCl, and 0.05% (w/v) FOS-CHOLINE®-15. Purification of recombinant ETR1 and RTE1 was examined by SDS-PAGE on 12 or 15% polyacrylamide gels (39) and visualized by silver staining (40) (supplemental data Fig. S2).

Tryptophan Fluorescence Spectroscopy—Quenching of steady-state tryptophan fluorescence was measured with a LS-55 Luminescence spectrophotometer (Perkin Elmer) at an excitation wavelength of 295 nm. Measurements were carried out with 0.2 μM of the purified recombinant RTE1 at 20 °C in a Quartz SUPRASIL macro/semi-micro cuvette (Perkin Elmer) containing 30 mM Tris-HCl, pH 7.5, 180 mM NaCl, 10 mM KCl, 0.05% (w/v) FOS-CHOLINE®-15, 0.1% (w/v) β-D-dodecylmaltoside, and 0.002% (w/v) PMSF. Purified trypto-

phan-less ETR1 dissolved in 50 mM Tris, pH 7.5, 50 mMNaCl and 0.1% (w/v) β-D-dodecylmaltoside was added up to a final concentration of 2 μM. The concentration-dependent quenching of the tryptophan fluorescence of RTE1 associated with the addition of the receptor protein was monitored at 352 nm. The dissociation constant of the RTE1-ETR1 complex was determined from the quenching data as described in Ref. 38.

RESULTS

Association of RTE1 and ETR1 Expressed Transiently in Tobacco Cells—We tested for physical association of *Arabidopsis* RTE1 and ETR1 in living tobacco cells using BiFC, which produces a fluorescent readout for protein-protein interaction through the reconstitution of yellow fluorescent protein (YFP) (41, 42). For RTE1, we constructed a *cYFP-RTE1* gene fusion expressing full-length RTE1 (amino acids 1–250) fused with a portion of YFP (residues 155–238, designated cYFP) (Fig. 1*A*). We fused cYFP at the N terminus of RTE1, because we previously found that RTE1 fused with red fluorescent protein (RFP) at the RTE1 N terminus was capable of rescuing the *rte1* mutant phenotype, whereas RTE1 carrying a C-terminal fusion to RFP was only partially functional (16). For ETR1, we constructed gene fusions expressing full-length ETR1 (amino acids 1–738) with YFP residues 1–154 (designated nYFP) fused at either the ETR1 N terminus or C terminus, creating *nYFP-ETR1* and *ETR1-nYFP*, respectively. The ETR1 N terminus is presumed to reside in the lumen, and the ETR1 C terminus in the cytoplasm (Fig. 1*A*), based on the known topology of a *Cucumismelo* ethylene receptor (43). All of the fusion constructs were placed under the control of the *CaMV 35S* promoter. The constructs were introduced into tobacco leaf epidermal cells by *Agrobacterium*-mediated infiltration for transient expression, and association of RTE1 with ETR1 was assayed in the epidermal cells based on the reconstitution of YFP fluorescence (BiFC). To facilitate expression of the transgenes, we co-infiltrated the tobacco leaves with *Agrobacterium* harboring the *p19* plasmid, which carries a gene-silencing suppressor (31). Infiltration of each construct alone (paired only with the *p19* plasmid) gave no fluorescence signal.

When *cYFP-RTE1* was assayed in combination with *nYFP-ETR1* (carrying nYFP fused to the N terminus of ETR1), no YFP fluorescence was detected (Table 1, data not shown). In contrast, a strong YFP fluorescence signal was observed when *cYFP-RTE1* was co-transformed with *ETR1-nYFP* (carrying nYFP fused to the C terminus of ETR1), indicating that RTE1 and ETR1 can physically associate *in vivo* (Fig. 1 and Table 1). The fluorescence pattern was reticulate, similar to that of *Arabidopsis* ETR1-GFP expressed in tobacco epidermal cells (15), suggesting proper subcellular localization of the interaction. The positive signal also suggested that the N terminus of RTE1 most likely lies in the cytoplasm where the C terminus of ETR1 is thought to reside (Fig. 1*A*). Treating the infiltrated plants with ethylene gas did not detectably enhance or block the fluorescence signal (data not shown).

We also assayed for interaction between cYFP-RTE1 and a truncated version of ETR1 (amino acids 1–349) carrying a C-terminal fusion to nYFP, since genetic evidence has suggested that RTE1 acts through ETR1 residues 1–349 (28). Fluorescence was still observed, although it was weaker than that seen with full-length ETR1 (Fig. 1*B* and Table 1).

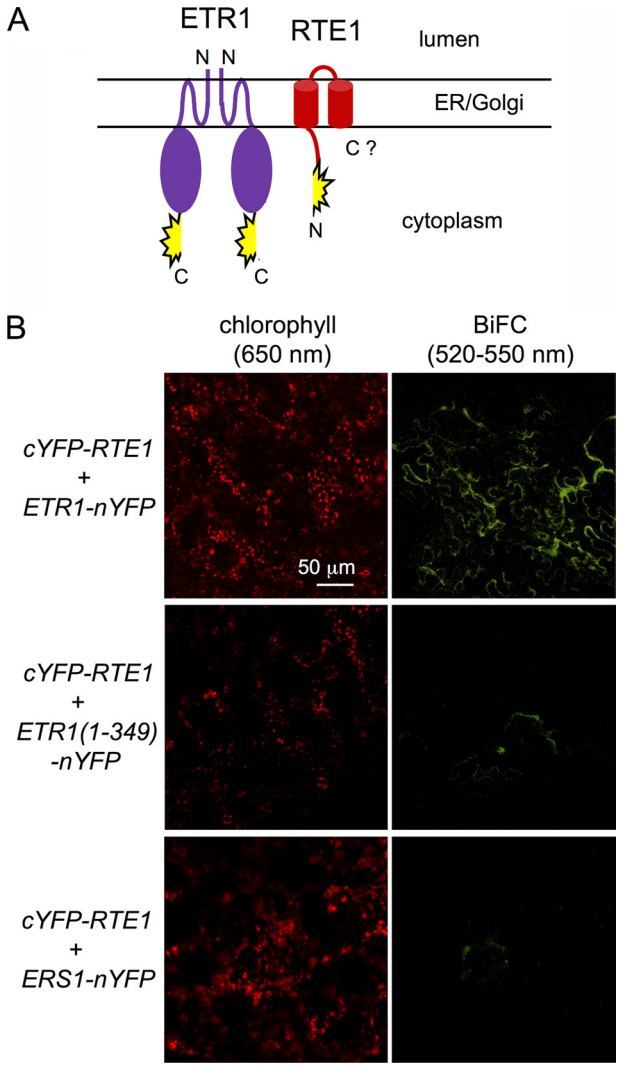

FIGURE 1. **BiFC visualization of RTE1 and ETR1 association in tobacco leaf epidermal cells.** *A*, schematic diagram of ETR1-nYFP and cYFP-RTE1 fusions showing their likely membrane topology. The *Arabidopsis* ETR1 ethylene receptor has three transmembrane domains and has nYFP (amino acids 1–154) fused to the ETR1 C terminus in the cytoplasm (43). *Arabidopsis* RTE1 has two to four predicted transmembrane domains (25) (two transmembrane domains are depicted) and has cYFP (aa 155–238) fused to the RTE1 N terminus. The cytoplasmic location of the RTE1 N terminus is deduced from the positive signal in *B*. The location of the RTE1 C terminus has not been determined. *B*, representative images from confocal laser scanning microscopy show chlorophyll autofluorescence (*left*) and reconstituted YFP fluorescence (*right*) in leaf epidermal cells of 3-week-old soil grown tobacco (*N. benthamiana*) 48 h after co-infiltration with *Agrobacterium* harboring *cYFP-RTE1* and either *ETR1-nYFP*, *ETR1(1–349)-nYFP*, or *ERS1-nYFP*. Scale bar, 50 μm.

To examine the specificity of the cYFP-RTE1 and ETR1-nYFP association, we assayed BiFC using another ER membrane-localized protein, ECA1 (a Ca^{2+}-ATPase, 44), in place of ETR1. Because ECA1 is a member of the highly conserved SERCA P-type ATPase family, its C terminus is expected to be cytoplasmic (45). No BiFC signal was detected for cYFP-RTE1 and ECA1-nYFP (Table 1 and data not shown). We also examined whether RTE1 can interact with ERS1, which is the

TABLE 1

Summary of BiFC results

BiFC signal intensity is indicated by "+++", "++", and "+" for strong to weak intensity, and "0" for no signal detected. Signal intensity was assessed under the confocal laser-scanning microscope. Experiments were carried out in triplicate, with at least ten independent plant samples examined for each replicate.

cYFP construct	nYFP construct	Tobacco leaf epidermal cells	*Arabidopsis* root cells	*Arabidopsis* cotyledon epidermal cells
cYFP-RTE1	*ETR1-nYFP*	+++	++	+++
cYFP-RTE1	*nYFP-ETR1*	0	0	0
cYFP-RTE1	*ETR1(1-349)-nYFP*	+	+	0
cYFP-RTE1	*ECA1-nYFP*	0	0	0
cYFP-RTE1	*ERS1-nYFP*	+	+	0
cYFP-RTH	*ETR1-nYFP*	0	nd[a]	nd
cYFP-rte1-1	*ETR1-nYFP*	0	nd	nd
cYFP-RTE1	*etr1-2-nYFP*	++	nd	nd
cYFP-RTE1	*etr1-1-nYFP*	++	nd	nd

[a] nd, not determined.

receptor most closely related to ETR1 (67% overall amino acid identity; 72% amino acid identity for residues 1–349). Using an ERS1 ethylene receptor carrying a C-terminal fusion to nYFP, a weak signal was detected (Fig. 1*C* and Table 1), suggesting that RTE1 might be capable of associating with ERS1. We also examined whether mutations in ETR1 could have an effect on the interaction with RTE1. We tested two gain-of-function mutations, *etr1-1* and *etr1-2*, which both confer ethylene insensitivity in *Arabidopsis*; *etr1-2* requires *RTE1* for ethylene insensitivity, whereas *etr1-1* is independent of *RTE1* (25). Despite this functional difference, both *etr1-1-nYFP* and *etr1-2-nYFP* showed interaction with *cYFP-RTE1*, although the interaction appeared to be weaker than with wild-type ETR1 (Fig. 2 and Table 1).

Conversely, we assayed the ETR1-nYFP fusion for interaction with the *Arabidopsis* RTE1 homolog, RTH (25), which has 51% identity to RTE1 over 209 amino acids and localizes to the same subcellular organelles as RTE1.[3] Despite the similarities between RTE1 and RTH, co-infiltration of *cYFP-RTH* and *ETR1-nYFP* gave no BiFC signal (Table 1 and data not shown), suggesting that the signal produced by *ETR1-nYFP* paired with *cYFP-RTE1* might be specific to RTE1.

BiFC of RTE1 and ETR1 in Stably Transformed Arabidopsis—The association of RTE1 and ETR1 was also visualized in *Arabidopsis*. *Arabidopsis* was stably transformed with each of the following binary constructs, all driven by the *CaMV 35S* promoter: *cYFP-RTE1*, *ETR1-nYFP*, *ETR1(1–349)-nYFP*, *ERS1-nYFP*, *ECA1-nYFP*, and *nYFP-ETR1*. Homozygous lines were generated for each transgene, and then genetically crossed to produce F1 progeny. BiFC was examined in the epidermal cells of roots and cotyledons of 1-week-old F1 seedlings. Consistent with the tobacco epidermal cell results, transgenic F1 progeny harboring both *cYFP-RTE1* and *ETR1-nYFP* produced detectable BiFC signals in both root and cotyledon epidermal cells (Fig. 3 and Table 1), while a weak signal was detected only in root cells (with no signal in cotyledon cells) when *cYFP-RTE1* was paired with either *ETR1(1–349)-nYFP* or *ERS1-nYFP* (Table 1 and data not shown). Unfortunately we were unable to detect the various fusion proteins when we carried out Western blotting to assess their expression levels (data not shown). Thus it is important to note that the BiFC signal strength does not necessarily correlate with protein-protein interaction strength.

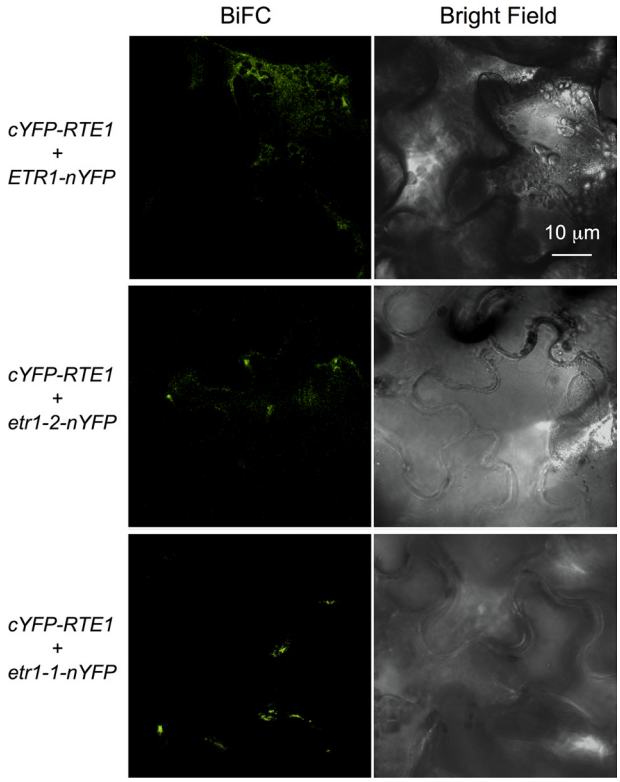

FIGURE 2. **BiFC assay for mutant versions of ETR1.** Representative images from confocal laser scanning microscopy show reconstituted YFP fluorescence (*left*) and DIC (*right*) in tobacco leaf epidermal cells co-infiltrated with *Agrobacterium* harboring *cYFP-RTE1* and either *ETR1-nYFP*, *etr1-2-nYFP*, or *etr1-1-nYFP*. Scale bar, 10 μm.

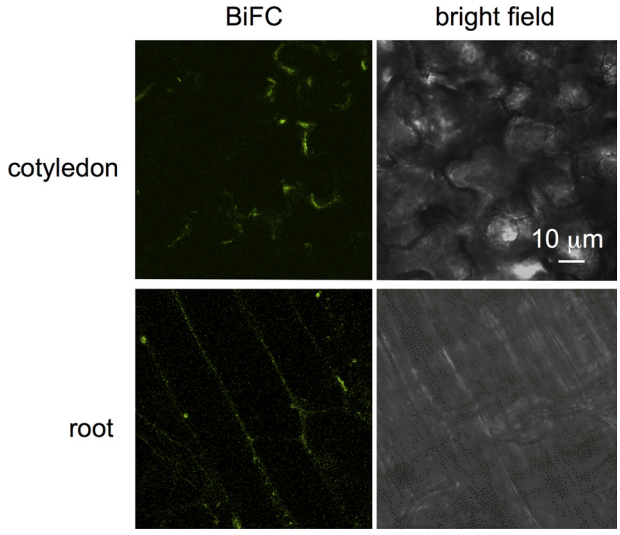

FIGURE 3. **BiFC visualization of RTE1 and ETR1 association in stably transformed *Arabidopsis*.** Representative images from confocal laser scanning microscopy show reconstituted YFP fluorescence (*left*) and bright field with Nomarski differential interference contrast (*DIC*) (*right*) in cotyledon and root cells of 1-week-old *Arabidopsis* plants expressing the *ETR1-nYFP* and *cYFP-RTE1*transgenes. Scale bar, 10 μm.

Co-IP of RTE1 and ETR1 in Stably Transformed Arabidopsis—To confirm the association of RTE1 and ETR1, we carried out co-IP using epitope-tagged versions of RTE1 and ETR1 expressed in stably transformed *Arabidopsis*. RTE1 was tagged at its N terminus with an HA epitope. A homozygous transgenic line expressing *HA-RTE1* (driven by the

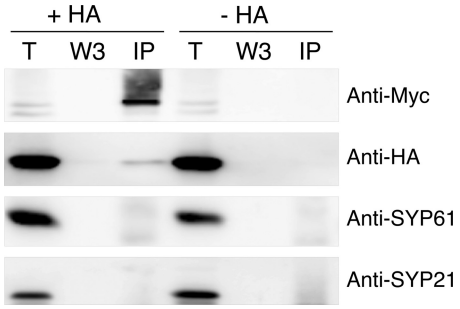

FIGURE 4. **Co-IP of RTE1 and ETR1.** Protein extracts of 3-day-old dark-grown F1 seedlings from genetic crosses of stably transformed *Arabidopsis* carrying ETR1–5xMyc and HA-RTE1, respectively, were subjected to immunoprecipitation using an anti-HA antibody (+*HA*). Total protein extracts (10%) (*T*), the third wash (*W3*) and the immunoprecipitates (*IP*) were separated by SDS-PAGE followed by immunoblotting using anti-c-Myc and anti-HA antibodies to detect ETR1–5xMyc and HA-RTE1, respectively. As a negative control, anti-SYP61 and anti-SYP21 antibodies were used to detect SYP61 (36) and SYP21 (35), which are transmembrane proteins localized to the trans-Golgi network and prevacuolar compartment, respectively. As an additional control, immunoprecipitation was performed in the absence of the primary anti-HA antibody (−*HA*).

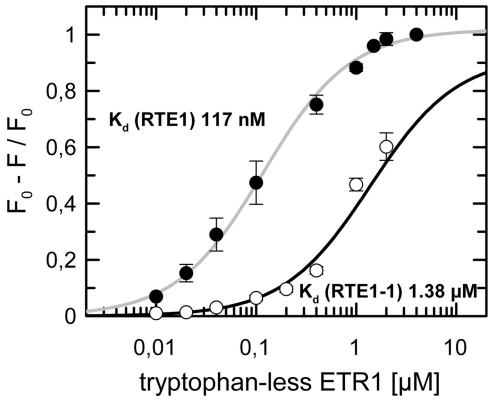

FIGURE 5. **Dissociation constant of the RTE1-ETR1 complex and the effect of the *rte1-1* mutation.** Complex formation of RTE1 and ETR1 was monitored by fluorescence spectroscopy. Binding partners were cloned and expressed in *E. coli* and purified from the bacterial host. Quenching in tryptophan fluorescence of purified RTE1 or RTE1-1 caused by the addition of recombinant tryptophan-less ETR1 was analyzed according to Ref. 38. The effect of the RTE1-1 mutant protein on complex formation with ETR1 is shown in comparison to that of wild-type RTE1. F_0 corresponds to the initial fluorescence intensities of the purified recombinant RTE1, F to the fluorescence obtained when different concentrations of the tryptophan-less ETR1 have been added. Data were fitted to a model assuming a single binding site in the interacting partners. The curves represent non-linear least squares fits obtained by GraFit (Erithacus Software Ltd.) and correspond to a dissociation constant of 117 nM ± 9 nM ($\chi^2 = 0.000584$) for RTE1 and 1.38 µM ± 0.62 µM ($\chi^2 = 0.0523$) for the RTE1-1 mutant.

CaMV 35S promoter) was crossed with a previously generated transgenic line expressing a functional ETR1–5xMyc fusion under the control of the native ETR1 promoter (16). The resulting F1 progeny expressing both HA-RTE1 and ETR1–5xMyc were used for co-IP. Total protein extracts were first incubated with or without anti-HA antibody, followed by precipitation with protein A-Sepharose. The immunoprecipitated fraction was run on a polyacrylamide gel and immunoblotting using an anti-c-Myc antibody showed the presence of ETR1–5xMyc only when the anti-HA antibody was used (Fig. 4). In contrast, the anti-HA antibody did not result in IP of SYP61 (a SNARE protein) (36) or SYP21 (syntaxin) (35), which are transmembrane proteins localized to the trans-Golgi network and prevacuolar compartment, respectively, thus demonstrating the specificity of the anti-HA co-IP. Co-IP of ETR-5xMyc was detected in three independent experiments, thus confirming the *in vivo* protein association of RTE1 and ETR1. Similar results were obtained for the reciprocal experiment, using anti-c-Myc for the co-IP (data not shown); however the anti-c-Myc antibody gave nonspecific background in Western blotting, so the specificity of the IP could not be ensured.

Quantitative Analysis of the RTE1-ETR1 Interaction by Tryptophan Fluorescence Spectroscopy—We next tested whether the interaction of RTE1 and ETR1 could occur in the absence of other proteins. The interaction and stability of the RTE1-ETR1 binary complex was examined *in vitro* using tryptophan fluorescence quenching. Full-length RTE1 (supplemental Fig. S2) and ETR1 proteins were expressed in and purified from *E. coli*. Correct folding and structure of the purified recombinant RTE1 was indicated by circular dichroism (supplemental Fig. S3). For ETR1, we used an existing functional tryptophan-less version of ETR1, in which seven tryptophan residues were replaced with either phenylalanine or leucine residues (38). The tryptophan-less version was necessary to allow for the titration measurements of tryptophan fluorescence in the RTE1 protein. Titration of the purified RTE1 with the tryptophan-less ETR1 protein yielded an apparent K_d of ~117 nM (Fig. 5). This relatively low dissociation constant provided evidence of a high affinity interaction between RTE1 and ETR1.

Reduced Affinity of the RTE1-ETR1 Interaction Caused by the rte1-1 Mutation—The *Arabidopsis rte1-1* mutation, encoding a C161Y substitution, was previously isolated by genetic screening and confers an *etr1* loss-of-function phenotype (25). We tested whether the C161Y substitution has an effect on the molecular association of RTE1 and ETR1 using BiFC and tryptophan fluorescence spectroscopy. For BiFC, the *rte1-1* mutation was introduced into the *cYFP-RTE1* construct using *in vitro* site-directed mutagenesis. The resulting *cYFP-rte1-1* mutant version was assayed for BiFC with *ETR1-nYFP* in tobacco leaf epidermal cells. In contrast to the positive signal obtained for wild-type cYFP-RTE1 and ETR1-nYFP, no signal was detected for cYFP-RTE1-1 and ETR1-nYFP, suggesting that the *rte1-1* mutation reduces the RTE1-ETR1 interaction (Table 1 and data not shown).

To test the effect of the *rte1-1* mutation on the ETR1-RTE1 complex using tryptophan fluorescence spectroscopy, the full-length *RTE1* clone was mutagenized to encode the *rte1-1* (C161Y) substitution, and the resulting RTE1-1 product was expressed in and purified from *E. coli* (supplemental Fig. S2). Based on circular dichroism, there were no substantial secondary structure changes between the purified recombinant RTE1-1 mutant protein and the purified recombinant RTE1 wild-type protein (supplemental Fig. S2). Titration of the purified recombinant RTE1-1 mutant protein with the tryptophan-less ETR1 protein showed a nearly 12-fold increase in the dissociation constant of the ETR1-RTE1-1 complex (1.38 µM) compared with titration of the purified recombinant wild-type RTE1 (Fig. 5). This increase indicates a substantial

decrease in the interaction of both binding partners due to the single mutation in RTE1-1 (C161Y).

DISCUSSION

RTE1 is a novel protein conserved in plants and animals. In *Arabidopsis,* RTE1 negatively regulates ethylene signaling (25), but the molecular mechanism of this regulation is unknown. RTE1 and ETR1 are both transmembrane proteins that co-localize to the ER and Golgi apparatus (16). Genetic data suggest that RTE1 promotes the signaling state of the ETR1 ethylene receptor (26). Here, we demonstrate a physical association between RTE1 and ETR1 *in vivo* and *in vitro*. Our findings suggest that RTE1 action in ethylene signaling involves a direct interaction with ETR1.

We first detected association of RTE1 and ETR1 using BiFC in a transient assay in tobacco leaf epidermal cells. Subsequently, we detected the interaction in stably transformed *Arabidopsis* using both BiFC and co-IP. The BiFC signal was observed when the N terminus of RTE1 and the C terminus of ETR1 were fused to cYFP and nYFP, respectively. We had previously shown that fusing RFP and a 5xMyc epitope tag at these particular termini of RTE1 and ETR1, respectively, does not disrupt RTE1 or ETR1 function in *Arabidopsis* (16). The C terminus of ETR1 is very likely to be in the cytoplasm based on the topology of a melon ethylene receptor (43). RTE1 is predicted to have two to four transmembrane domains (25) but the membrane topology of RTE1 is unknown. We found that RTE1 lacks *N*-linked glycosylation,[3] precluding the use of *N*-linked glycosylation to determine the topology. Nevertheless, the positive BiFC signal produced by the combination of cYFP-RTE1 and ETR1-nYFP suggested that the N terminus of RTE1 lies on the cytoplasmic side of the membrane, which is where the C terminus of ETR1 is believed to reside. Moreover, the subcellular pattern of the BiFC signal was comparable to that of GFP-tagged ETR1. In addition, we obtained a BiFC signal for cYFP-RTE1 paired with ETR1(1–349)-nYFP. ETR1(1–349) has been shown to have the same subcellular localization as wild-type ETR1 (14). This is consistent with genetic data that indicates RTE1 promotes ETR1 signaling via the ETR1 N terminus (residues 1–349) (28).

The *in vivo* molecular interaction of RTE1 and ETR1 was confirmed by co-IP in *Arabidopsis*, and the affinity of the interaction was examined by tryptophan fluorescence quenching measurements, using purified RTE1 and ETR1 proteins expressed in *E. coli*. Association *in vitro* occurred with high affinity, based on the determined K_d value of ~117 nM. This low $K_d$value is indicative of a specific interaction, rather than a nonspecific interaction arising from hydrophobic interactions, and is comparable to that of other known, highly specific protein-protein interactions, such as NusB:S10 (46), the NusA:core RNA polymerase (47), Ras:Raf (48), and EGF:EGF receptor (49). This *in vitro* association suggests that the physical interaction of RTE1 and ETR1 does not require the presence of other plant proteins.

The *rte1-1* mutation encodes a C161Y substitution and confers an ethylene hypersensitive phenotype similar to the *etr1* loss-of-function phenotype. Significantly, we found that the *rte1-1* mutation reduces the affinity of the molecular association of RTE1 with ETR1, in both BiFC and fluorescence spectroscopy. The dissociation constant for the *in vitro* association was nearly 12-fold higher for the recombinant RTE1-1 mutant protein compared with the recombinant RTE1 wild-type protein. Thus, the physical interaction of ETR1 with RTE1 appears to be required to maintain ETR1 function.

BiFC signals were observed for wild-type RTE1 and the two dominant gain-of function mutants, *etr1-1* and *etr1-2,* even though *etr1-1* signaling is independent of *RTE1*. This suggests that the *RTE1* independence of the *etr1-1* allele is not due to a loss of association between ETR1-1 and RTE1. Perhaps the particular conformation of ETR1-1, or an interacting protein, is the basis for its *RTE1* independence.

Although genetic analysis indicates that RTE1 specifically acts on ETR1 and not on the other *Arabidopsis* ethylene receptors (25, 27, 28), we also detected a weak signal for cYFP-RTE1 paired with ERS1-nYFP, which suggests that RTE1 might interact to some extent with the ERS1 receptor. Given that ERS1 and ETR1 are likely to be in contact with each other in the ethylene receptor complex (23), it is conceivable that there was reconstitution of the BiFC signal based on close proximity of the YFP halves, or that there is actually a nonfunctional interaction of RTE1 and ERS1. The absence of detectable interaction between cYFP-RTH (the RTE1 homolog) and ETR1-nYFP is consistent with data suggesting that the RTE1 homolog, RTH, does not play the same role as RTE1 in ethylene signaling.[3]

The physical association of RTE1 and ETR1 is consistent with the highly specific functional interaction of RTE1 and ETR1 that has been suggested by genetic analyses. RTE1 and ETR1 have possibly co-evolved, as implicated by their physical and functional association. This is interesting in light of the fact that RTE1 is present not only in plants, but is conserved in metazoans and some fungi. Because these other organisms are not known to encode ethylene receptors, RTE1 homologs might possess a more general conserved cellular function.

Acknowledgments—We thank Prof. Klaus Harter and Universität Tübingen (Germany) for generously providing pSPYNE-35S-GW and pSPYNE-35S/pUC-SPYNE, VIB (Belgium) for providing pH2GW7, PBL (UK) for providing Agrobacterium strain C58C1 (pCH32) and p19, ABRC (The Ohio State University) for providing pEARLEYGATE201, Dr. Natasha Raikhel (University of California, Riverside) for providing the anti-SYP21 and anti-SYP61 antibodies, Dr. Heven Sze (University of Maryland, College Park) for providing the ECA1 cDNA clone, Amy Beaven of the Imaging Core Facility (CBMG Dept., University of Maryland, College Park) for confocal microscopy support, W. Hunter Tuck for construction of the nYFP-etr1-1 clone, Melanie Bisson, Jennifer Shemansky, and Andrew Scaggs for technical assistance, and J. Shemansky for comments on the manuscript.

REFERENCES

1. Abeles, F. B., Morgan, P. W., and Saltveit, M. E. (1992) *Ethylene in Plant Biology*, 2nd Ed., Academic Press, San Diego, CA
2. Kendrick, M. D., and Chang, C. (2008) *Curr. Opin. Plant Biol.* **11,** 479–485
3. Stepanova, A. N., and Alonso, J. M. (2009) *Curr. Opin. Plant Biol.* **12,** 548–555

4. Chang, C., Kwok, S. F., Bleecker, A. B., and Meyerowitz, E. M. (1993) *Science* **262,** 539–544
5. Hua, J., Chang, C., Sun, Q., and Meyerowitz, E. M. (1995) *Science* **269,** 1712–1714
6. Sakai, H., Hua, J., Chen, Q. G., Chang, C., Medrano, L. J., Bleecker, A. B., and Meyerowitz, E. M. (1998) *Proc. Natl. Acad. Sci. U.S.A.* **95,** 5812–5817
7. Hua, J., Sakai, H., Nourizadeh, S., Chen, Q. G., Bleecker, A. B., Ecker, J. R., and Meyerowitz, E. M. (1998) *Plant Cell* **10,** 1321–1332
8. Wang, W., Hall, A. E., O'Malley, R., and Bleecker, A. B. (2003) Proc. *Natl. Acad. Sci. U.S.A.* **100,** 352–357
9. Hall, A. E., and Bleecker, A. B. (2003) *Plant Cell* **15,** 2032–2041
10. Qu, X., Hall, B. P., Gao, Z., and Schaller, G. E. (2007) *BMC Plant Biol.* **7,** 3
11. Schaller, G. E., and Bleecker, A. B. (1995) *Science* **270,** 1809–1811
12. Hall, A. E., Findell, J. L., Schaller, G. E., Sisler, E. C., and Bleecker, A. B. (2000) *Plant Physiol.* **123,** 1449–1458
13. O'Malley, R. C., Rodriguez, F. I., Esch, J. J., Binder, B. M., O'Donnell, P., Klee, H. J., and Bleecker, A. B. (2005) *Plant J.* **41,** 651–659
14. Chen, Y. F., Randlett, M. D., Findell, J. L., and Schaller, G. E. (2002) *J. Biol. Chem.* **277,** 19861–19866
15. Grefen, C., Städele, K., R[ring]uzicka, K., Obrdlik, P., Harter, K., and Horák, J. (2008) *Mol. Plant* **1,** 308–320
16. Dong, C. H., Rivarola, M., Resnick, J. S., Maggin, B. D., and Chang, C. (2008) *Plant J.* **53,** 275–286
17. Gamble, R. L., Coonfield, M. L., and Schaller, G. E. (1998) *Proc. Natl. Acad. Sci. U.S.A.* **95,** 7825–7829
18. Moussatche, P., and Klee, H. J. (2004) *J. Biol. Chem.* **279,** 48734–48741
19. Voet-van-Vormizeele, J., and Groth, G. (2008) *Mol. Plant* **1,** 380–387
20. Hua, J., and Meyerowitz, E. M. (1998) *Cell* **94,** 261–271
21. Wang, W., Esch, J. J., Shiu, S. H., Agula, H., Binder, B. M., Chang, C., Patterson, S. E., and Bleecker, A. B. (2006) *Plant Cell* **18,** 3429–3442
22. Schaller, G. E., Ladd, A. N., Lanahan, M. B., Spanbauer, J. M., and Bleecker, A. B. (1995) *J. Biol. Chem.* **270,** 12526–12530
23. Chen, Y. F., Gao, Z., Kerris, R. J., 3rd, Wang, W., Binder, B. M., and Schaller, G. E. (2010) *PLoS One* **5,** e8640
24. Gao, Z., Wen, C. K., Binder, B. M., Chen, Y. F., Chang, J., Chiang, Y. H., Kerris, R. J., 3rd, Chang, C., and Schaller, G. E. (2008) *J. Biol. Chem.* **283,** 23801–23810
25. Resnick, J. S., Wen, C. K., Shockey, J. A., and Chang, C. (2006) *Proc. Natl. Acad. Sci. U.S.A.* **103,** 7917–7922
26. Resnick, J. S., Rivarola, M., and Chang, C. (2008) *Plant J.* **56,** 423–431
27. Rivarola, M., McClellan, C. A., Resnick, J. S., and Chang, C. (2009) *Plant Physiol.* **150,** 547–551
28. Zhou, X., Liu, Q., Xie, F., and Wen, C. K. (2007) *Plant Physiol.* **145,** 75–86
29. Barry, C. S., and Giovannoni, J. J. (2006) *Proc. Natl. Acad. Sci. U.S.A.* **103,** 7923–7928
30. Clough, S. J., and Bent, A. F. (1998) *Plant J.* **16,** 735–743
31. Voinnet, O., Rivas, S., Mestre, P., and Baulcombe, D. (2003) *Plant J.* **33,** 949–956
32. Karimi, M., Inzé, D., and Depicker, A., (2002) *Trends Plant Sci.* **7,** 193–195
33. Walter, M., Chaban, C., Schütze, K., Batistic, O., Weckermann, K., Näke, C., Blazevic, D., Grefen, C., Schumacher, K., Oecking, C., Harter, K., and Kudla, J. (2004) *Plant J.* **40,** 428–438
34. Earley, K. W., Haag, J. R., Pontes, O., Opper, K., Juehne, T., Song, K., and Pikaard, C. S. (2006) *Plant J.* **45,** 616–629
35. Da Silva Conceição, A., Marty-Mazars, D., Bassham, D. C., Sanderfoot, A. A., Marty, F., and Raihkel, N. V. (1997) *Plant Cell* **9,** 571–582
36. Sanderfoot, A. A., Kovaleva, V., Bassham, D. C., and Raikhel, N. V. (2001) *Mol. Biol. Cell* **12,** 3733–3743
37. Scharein, B., Voet-van-Vormizeele, J., Harter, K., and Groth, G. (2008) *Anal. Biochem.* **377,** 72–76
38. Bisson, M. M., Bleckmann, A., Allekotte, S., and Groth, G. (2009) *Biochem. J.* **424,** 1–6
39. Laemmli, U. K. (1970) *Nature* **227,** 680–685
40. Heukeshoven, J., and Dernick, R. (1988) *Electrophoresis* **9,** 28–32
41. Bracha-Drori, K., Shichrur, K., Katz, A., Oliva, M., Angelovici, R., Yalovsky, S., and Ohad, N. (2004) *Plant J.* **40,** 419–427
42. Citovsky, V., Gafni, Y., and Tzfira, T. (2008) *Methods* **45,** 196–206
43. Ma, B., Cui, M. L., Sun, H. J., Takada, K., Mori, H., Kamada, H., and Ezura, H. (2006) *Plant Physiol.* **141,** 587–597
44. Liang, F., Cunningham, K. W., Harper, J. F., and Sze, H. (1997) *Proc. Natl. Acad. Sci. U.S.A.* **94,** 8579–8584
45. Lewin, B., Cassameris, L., Lingappa, V. R., and Plopper, G. (2007) *Cells*, pp. 73–74, Jones & Bartlett Learning, Sudbury, MA
46. Mason, S. W., Li, J., and Greenblatt, J. (1992) *J. Mol. Biol.* **223,** 55–66
47. Greenblatt, J., and Li, J. (1981) *Cell* **24,** 421–428
48. Warne, P. H., Viciana, P. R., and Downward, J. (1993) *Nature* **364,** 352–355
49. Zhou, M., Felder, S., Rubinstein, M., Hurwitz, D. R., Ullrich, A., Lax, I., and Schlessinger, J. (1993) *Biochemistry* **32,** 8193–8198